

# Gauge Field and Confinement-Deconfinement Transition in Hydrogen-bonded ferroelectrics

Chyh-Hong Chern<sup>1</sup> and Naoto Nagaosa<sup>2,3</sup>

<sup>1</sup>*Department of Physics, National Taiwan University, Taipei 10617, Taiwan*

<sup>2</sup>*Department of Applied Physics, University of Tokyo, Tokyo 113-8656, Japan*

<sup>3</sup>*Cross Correlated Materials Research Group (CMRG) and Correlated Electron Research Group (CERG), ASI, RIKEN, Wako 351-0198, Japan*  
(Dated: January 22, 2013)

Quantum melting of ferroelectric moment in the frustrated hydrogen-bonded system with "ice rule" is studied theoretically by using the quantum Monte Carlo simulation. The large number of nearly degenerate configurations are described as the gauge degrees of freedom, i.e., the model is mapped to a lattice gauge theory which shows the confinement-deconfinement transition (CDT). The dipole-dipole interaction  $J_2$ , on the other hand, explicitly breaks the gauge symmetry leading to the ferroelectric transition (FT). It is found that the crossover from FT to CDT manifests itself in the reduced correlation length of the polarization  $\xi_{\text{FT}} \sim \Delta(K - K_c)^{-\nu}$  with  $\Delta \propto \sqrt{J_2}$  while  $K_c$  and  $\nu$  remains finite in the limit  $J_2 \rightarrow 0$ . In contrast, the susceptibility  $\chi$  and the spontaneous polarization continues smoothly in this limit. Moreover, CDT is related to the shape or volume of the molecules, and the its correlation length  $\xi_{\text{CDT}}$  is not reduced in the limit of  $J_2 \rightarrow 0$ . A proposal for the neutron scattering or X-ray and Raman experiments is given to confirm this prediction.

PACS numbers: 64.70.K-, 64.60.-i, 11.15.-q

The hydrogen-bonded systems are one of the ideal laboratories to study the quantum tunneling. Especially, the ferroelectric properties of these systems attract much attention since the old work by Slater on KDP [1]. The quantum melting of the ferroelectric order to result in the quantum paraelectricity is a rather common phenomenon observed in several hydrogen-bonded ferroelectrics [2–5], which is usually described by the transverse Ising model as given by

$$H = - \sum_{ij} J_{ij} \sigma_i^z \sigma_j^z - K \sum_i \sigma_i^x, \quad (1)$$

where  $\sigma^z = \pm 1$  specifies the two positions of the hydrogen atoms,  $J_{ij}$  is the dipole-dipole interaction, and  $K$  represents the tunnelling matrix element. These two interactions compete with each other, and by increasing  $K$ , there occurs a phase transition from the ordered state to the quantum disordered phase. It is well known that the model Eq.(1) in  $d$ -spatial dimensions at zero temperature is equivalent to the  $(d+1)$ -dimensional classical Ising model at finite temperature  $T$  with  $K$  playing the role of  $T$  [6, 7].

On the other hand, it often happens that the constraints are significant to the hydrogen-bonded systems. Actually, the hydrogen positions in the representative system KDP are already subject to the constraint, i.e., so called "ice rule" [1]. Namely, only two of the four hydrogen atoms next to a tetrahedron are approaching to the center for the low energy sector. Similar constraint is also relevant to the recently studied quasi-two dimensional antiferroelectric squaric acid, where the square molecule is surrounded by 4 molecules with hydrogen bonds [5], and the two-in-two-out configurations are energetically stable. This "ice rule" is the generalization of the hydrogen bonds in ice leading to the macroscopic degeneracy of the ground state configurations as discussed by Pauling long time ago [8]. Therefore, a keen issue is how this macroscopic degeneracy of the low energy states affects the physical properties of the hydrogen bonded systems, which we address in this paper.

The constraints imposed on the physical variables are more common phenomenon found in many other cases. Frustrated magnets are one of such examples, where some of the macroscopically degenerate spin configurations are selected as the lowest energy states. Spin ice in pyrochlore ferromagnet is a representative example, in which the hydrogen position is replaced by the direction of the spin, and the "ice rule" is applied here also. This fact leads to an interesting phenomena, e.g., the absence of the long range ordering down to zero temperature and the deconfined magnetic monopoles as the excitations [9]. These are described well by the gauge theory representing the constraints within the framework of the classical statistical mechanics. Quantum effects on the spin ice model have been attracting intense interests recently [10, 11].

In this paper, we study theoretically the phase transition in a (2+1)-dimensional model of the hydrogen-bonded ferroelectrics with the ice rule. This model shows two types of phase transitions, i.e., the confinement-deconfinement transition (CDT) and the ferroelectric transition (FT), and the issue is how these two are connected. As discussed below, the latter is induced by the dipole-dipole interaction  $J_2$  which explicitly breaks the gauge symmetry, while the former exists with the pure gauge model.

Inspired by the squaric acid, we consider the following model

$$H = H_0 + H_1 + H_2, \quad (2)$$

where

$$H_0 = -J_0 \sum_{\square} \sigma_1^z \sigma_2^z \sigma_3^z \sigma_4^z - K \sum_i \sigma_i^x, \quad (3)$$

$$H_1 = J_1 \sum_{\square} (\sigma_1^z \sigma_3^z + \sigma_2^z \sigma_4^z), \quad (4)$$

$$H_2 = -J_2 \sum_{\langle AB \rangle} \vec{P}_A \cdot \vec{P}_B. \quad (5)$$

in the lattice given in Fig. 1A. The summation of  $\square$  in Eq. (3)

and (4) is over the blue plaquettes which resemble the  $H_2SQ$  molecules [5]. The sites are labeled by numbers and the convention is given in Fig. 1A. On each site, there is a hydrogen shared by two neighboring molecules, representing the hydrogen bond.  $\sigma^z$  is used to denote the motion of protons: If a hydrogen is closer to the plaquette of group A, it is defined as the "+" state, otherwise it is a "-" state. The summation in Eq. (5) is over the nearest-neighbor plaquettes, and  $\bar{P}_i$  are defined as the following

$$P_{Ax} = \frac{1}{4}(\sigma_1^z + \sigma_2^z - \sigma_3^z - \sigma_4^z), \quad (6)$$

$$P_{Ay} = \frac{1}{4}(\sigma_2^z + \sigma_3^z - \sigma_1^z - \sigma_4^z) \quad (7)$$

for the plaquettes of group A, and

$$P_{Bx} = \frac{1}{4}(\sigma_3^z + \sigma_4^z - \sigma_1^z - \sigma_2^z), \quad (8)$$

$$P_{By} = \frac{1}{4}(\sigma_1^z + \sigma_4^z - \sigma_2^z - \sigma_3^z) \quad (9)$$

for the plaquettes of group B, representing the polarization vectors.

The model described by  $H_0$  only is nothing but the quantum Hamiltonian of the (2+1)-dimensional Ising gauge theory, where  $\sigma^z$  is the bond variable of the dual lattice illustrated by the dash plaquette in Fig. 1A. It is well known that it is dual to a three-dimensional classical Ising model. When  $K = 0$ , it becomes a two-dimensional Ising gauge theory dual to the one-dimensional Ising model [6, 7]. There is macroscopic ground state degeneracy. In each plaquette, there are 8 different configurations in the low energy sector illustrated in Fig. 1B. The addition of  $H_1$  lifts the degeneracy so that the states of (e) to (h) are favored. States (e) to (h) are particularly interesting because they carry finite dipole moments. The direction of the dipole moments for the plaquettes of group A are shown in red arrows in Fig. 1B. Finally, a nearest-neighbor dipole interaction is introduced by  $H_2$ .

Let us consider the classical model first, namely  $K = 0$ . The finite-temperature phase diagram is summarized in Fig. 2. For  $J_1 = J_2 = 0$ , the system is always disordered, since the model is equivalent to a one-dimensional Ising model by an appropriate gauge choice, i.e., there is no phase transition at finite temperature. For  $J_1 \gg J_0$  and  $J_2 = 0$ , the gauge symmetry is partially broken. Namely, the model becomes infinite number of decoupled one-dimensional antiferromagnetic Ising chains, and is again equivalent to the 2D Ising gauge model. Therefore, the system is still disordered without finite-temperature phase transition. This can be explicitly shown by introducing the  $\eta$  variables defined in the dual lattice, for example  $\sigma_2^z = \eta_i \eta_j$  as shown in Fig. 1A. Then, to minimize the energy for  $H_0$ , the Hamiltonian  $H$  at  $J_2 = 0$  is given by

$$H = -J_0 + 2J_1 \sum_{\square} \eta_i \eta_j \eta_k \eta_l, \quad (10)$$

where  $\square$  is the spatial plaquettes in the dual lattice. The effective Hamiltonian of Eq. (10) is a classical 2-dimensional Ising

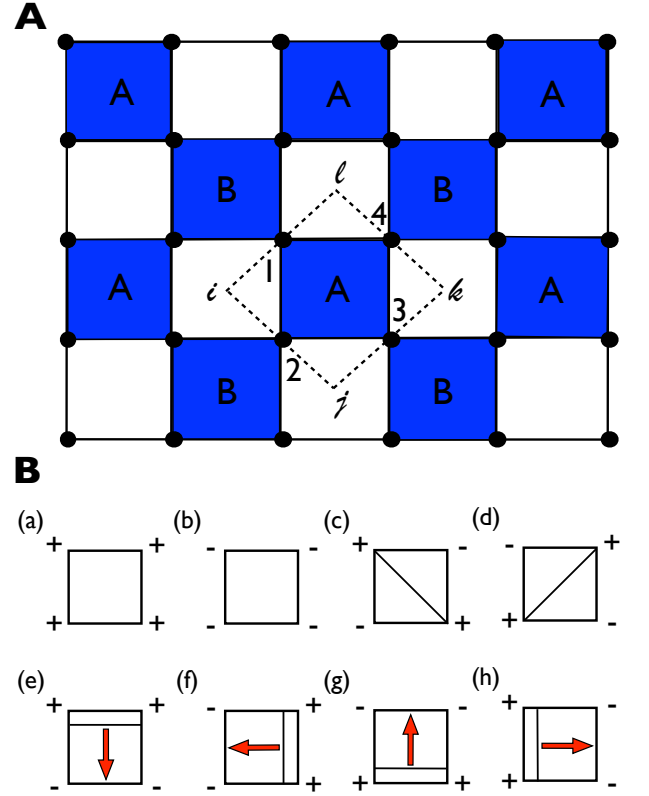


FIG. 1: (A) The squaric acid is layered structure, and  $H_2SQ$  molecules span a two-dimensional network marked in blue. The black dots denote the hydrogen sites. We divide them into two groups to define the dipole moment. If the hydrogen is closer to (away from) the molecules of group A (B), it is a "+" state, otherwise it is a "-" state. The dual lattice is drawn in dash lines. (B) The ground state configuration of each plaquette in the model of  $H_0$  only. There are no dipole moment in the states (a) to (d), and there are finite dipole moments in the states (e) to (h). The directions of the dipole moment are drawn in red for the molecules of group A.

gauge theory as mentioned above. Therefore, for  $J_2 = 0$  and  $K = 0$ , it is in the disordered phase over all temperature range shown as the pink region in Fig. 2. For  $J_2 \neq 0$ ,  $H_2$  introduces a two-dimensional Ising model, which breaks explicitly the gauge invariance. There is a ferroelectric phase transition at finite temperature. For small  $J_2$ , the transition temperature  $T_c$  behaves like  $\sim J_1 / \log(J_1/J_2)$  for  $J_1 \gg J_0$ , which vanishes as  $J_2$  goes to zero.

Now let us turn to the quantum model. For  $K \neq 0$ , the zero-temperature phase diagram can be summarized in Fig. 3. When  $J_1 = J_2 = 0$ , there is a confinement-deconfinement transition (CDT) at critical  $K_c$ . Since the model is dual to a (2+1)-dimensional Ising model, the CDT is a second order phase transition [6, 7]. In order to demonstrate whether or not the CDT extends to finite  $J_1$  region (at  $J_2 = 0$ ), we perform the quantum Monte Carlo calculation in addition to the analysis using the  $\eta$  variables. The numerical results, organised in the Supplementary Information, indicate that the second-order quantum phase transition extends to finite  $J_1$  re-

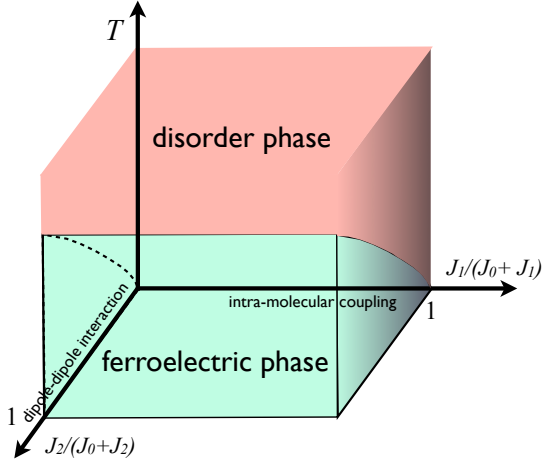


FIG. 2: Finite temperature phase diagram of the classical model for  $K = 0$ . The disorder phase is drawn in pink, and the ferroelectric phase is drawn in green.  $J_1$  is the intra-molecular coupling, and  $J_2$  is the dipole-dipole interaction.

gion, which is consistent with the  $\eta$ -variable analysis. The consistency is not surprising since the model behaves like a one-dimensional transverse-field Ising model in the  $J_1 \rightarrow \infty$  limit, where there is a second-order quantum phase transition separating the phase with critical correlation and the classical paramagnetic phase. The CDT extends to the finite  $J_1$  region and continues smoothly to the quantum phase transition at  $J_1 = \infty$ . As a short summary shown in Fig. 3, on the  $J_2 = 0$  plane, the phase diagram is divided into two regions. One is the deconfined phase and the other is the confined phase.

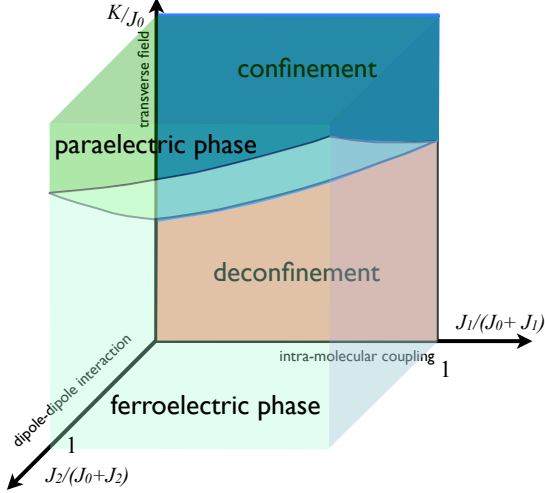


FIG. 3: The quantum phase diagram of Eq. (2). For  $J_2 = 0$ , there are two phases separated by a confinement-deconfinement phase transition. For finite  $J_2$ , the phase space is divided by a second-order ferroelectric phase transition.

Introducing the dipole-dipole interaction  $J_2 \neq 0$ , the ground state develops a spontaneous polarization at small transverse field  $K$ . A quantum phase transition to the para-

electric state can be driven by  $K$ . In Fig. 4, the dielectric constant is computed for 5 different values of  $J_2$ . In Fig. 5, we show the results of the correlation length  $\xi_{\text{FT}}$  for the dipole moments for  $K > K_c$ . The ferroelectric transition is a second-order phase transition because both dielectric constant and the correlation length diverge at  $K = K_c$ . Therefore, the phase space is divided into two regions for finite  $J_2$ : a ferroelectric phase and a paraelectric phase. Extending to the finite  $J_2$  region, the deconfined phase at the zero- $J_2$  plane becomes the ferroelectric phase, and the confined phase becomes the paraelectric phase as shown in Fig. 3. Due to these non-trivial connections, how does the criticality of the confinement-deconfinement phase transition (CDT) of the gauge field affect the criticality of the ferroelectric phase transition (FT) is the main scope of this paper.

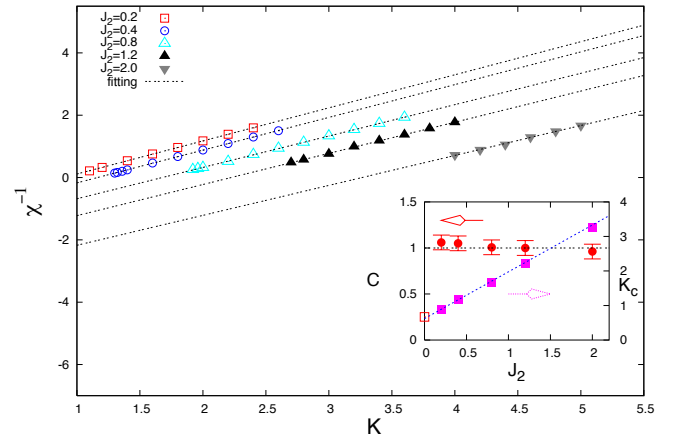


FIG. 4: The inverse of the dielectric susceptibility  $\chi^{-1}$  for  $J_2 = 0.2, 0.4, 0.8, 1.2, 2.0$  is computed for  $J_0 = 1$  and  $J_1 = 0.2$ . The dielectric susceptibility satisfies well the Curie-Weiss's law  $\chi = C/(K - K_c)$ . In the inset, we extract  $C$  and  $K_c$  as function of  $J_2$ . The curve in panel  $C$  uses the left  $y$ -axis, and the one for  $K_c$  uses the right  $y$ -axis.  $C$  is almost 1 independent of  $J_2$ , indicating the robustness of the ferroelectric transition for any finite  $J_2$ .  $K_c$  has a linear relation with  $J_2$ , terminating at  $K_c = 0.67$  for  $J_2 = 0$ , which is the  $K_c$  for the confinement-deconfinement phase transition.

As shown in Fig. 4, the dielectric susceptibility satisfies the Curie-Weiss's law  $\chi = C(K - K_c)^{-1}$  with  $C = 1$  for all  $J_2$ , where  $C$  carries the information of the square of the polarization moment. Our results indicate that the ferroelectric transition is robust for any finite  $J_2$ , i.e.,  $K_c$  converges to a finite value. As shown in Fig. 5A, the correlation length  $\xi$  obeys  $\xi_{\text{FT}} \sim \frac{\Delta}{(K - K_c)^\nu}$  very nicely with  $\nu = 0.46, 0.42, 0.41, 0.46, 0.55$  for  $J_2 = 0.2, 0.4, 0.8, 1.2, 2.0$ , remaining finite as approaching to  $J_2 = 0$ . We believe that the fluctuation of the  $\nu$  comes from error bars in the estimation. Using the field-theoretical technique, detailed in the Supplementary Information, we obtain

$$\Delta \sim \sqrt{\frac{J_2}{2J_2 + 4(2J_0 - J_1) + \lambda}}, \quad (11)$$

where  $\lambda$  is the Lagrange multiplier to impose the constraint of the fixed number of spin states. Our numerical results can be fitted well with the analytical result by a proportional constant 2.2 as shown in Fig. 5B. As the correlation length defines the critical region, our results indicate that the gauge field regulates the critical region as the system approaches to the critical point. Although the ferroelectric transition is robust for any finite  $J_2$ , the correlation vanishes as the system approaches to the CDT, consistent with Eq. (10) that any quantity which is not gauge invariant has the zero expectation value [6, 7]. This profound property provides a good measure of distance for a ferroelectric system in the vicinity of the CDT. The measurement of the correlation length by neutron scattering or X-ray scattering [12, 13] toward the phase transition point can provide a strong evidence that the system is near the CDT, i.e., the degree of frustration, in comparison with the susceptibility and spontaneous polarization, both of which do not show any special behaviour.

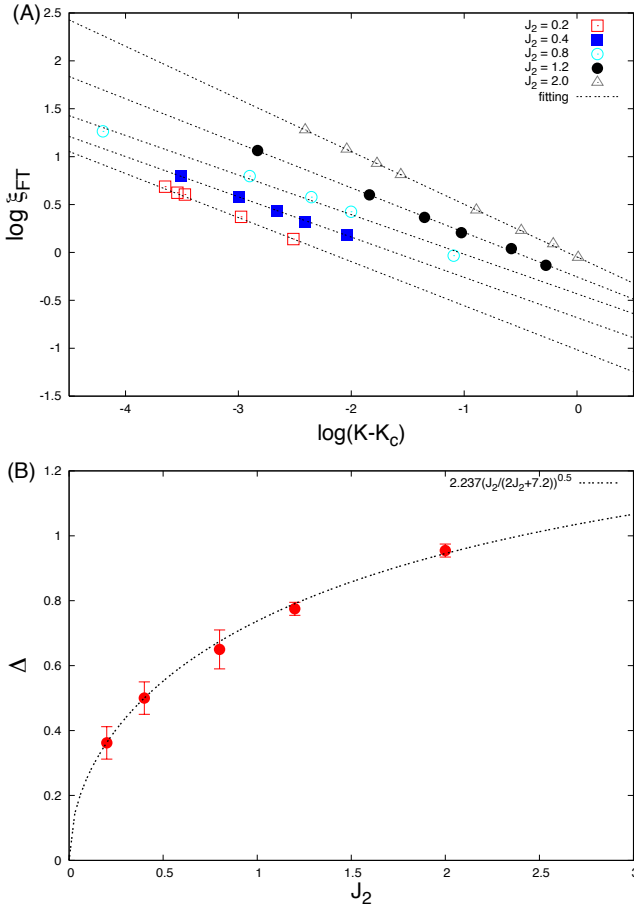


FIG. 5: (A) The log-log plot of the correlation length  $\xi$ .  $\nu$  are obtained as 0.55, 0.46, 0.41, 0.42, 0.46 for  $J_2 = 2.0, 1.2, 0.8, 0.4$ , and 0.2 respectively. As the dipole-dipole interaction  $J_2$  is switched on, the system immediately becomes an ordinary ferroelectric system. (B) The coefficient  $\Delta$  of the correlation length as the function of  $J_2$ . The blue-dot line is the fitting of the analytical result.

Next let us turn to the CDT. The order parameter for CDT is

intricate. It is a conventional local order parameter in the dual variable but a nonlocal order parameter in original  $\sigma$ 's. For simplicity, we consider below the case of  $J_1 = 0$ . The product of four  $\sigma^z$ 's around a plaquette  $i$ , i.e.,  $p_i = \sigma_1^z \sigma_2^z \sigma_3^z \sigma_4^z$ , is the gauge invariant and relevant quantity for CDT. Usually, the Wilson loop  $W(C) = \prod_i p_i$ , where the product over  $i$  runs over the all plaquettes inside the loop  $C$ , is the "order parameter" for CDT [6, 7]. However, this quantity is rather difficult to be related to a physical observable in the present case. Instead, we consider the correlation of  $p_i$ 's which shows the scaling behavior in the critical region as

$$\langle p_i p_j \rangle \sim R^{-(d-\alpha/\nu)} g(R/\xi_{CDT}), \quad (12)$$

where  $R = |R_i - R_j|$  is the distance between the two plaquettes  $i$  and  $j$ , while  $\alpha$  and  $\nu$  are the critical exponent for the specific heat and the correlation length, respectively. The function  $g$  is a scaling function and  $\xi_{CDT}$  is the correlation length of the dual 3D Ising model, which diverges as  $K$  approaches to  $K_c$  [7]. We expect the same critical exponent  $\nu$  for  $\xi_{CDT}$  as  $\xi_{FT}$  for the FT. However,  $\xi_{CDT}$  is not reduced in the limit of  $J_2 \rightarrow 0$ , which means that we have two correlation lengths  $\xi_{FT}$  and  $\xi_{CDT}$  for small  $J_2$ .

Now the question is how to detect  $\xi_{CDT}$  experimentally. It is noted here that  $p_i$  is concerned about the shape or volume of the molecule  $i$ . It is known that the change in the molecular shape results in the change in the frequencies of some molecular vibrations [12]. For simplicity, we consider the model where frequency of a molecular vibration  $\Omega_i$  depends on the plaquette variable as  $\Omega_i = \Omega_0 + ap_i$ . Then, we consider the Raman scattering spectrum due to this vibration mode, whose intensity  $I(q, \omega)$  is given by

$$I(q, \omega) \sim \int dt \int dt' \sum_{i,j} \langle e^{-iq \cdot (R_i - R_j)} e^{i(\omega(t-t') - \Omega_i t + \Omega_j t')} \rangle \quad (13)$$

where  $q$  is the momentum transfer between the incident and emitted lights and  $\omega$  is the Stokes shift. Assuming the Gaussian fluctuation for  $p_i$ 's in the coarse grained model, we can obtain

$$I(q, \omega) \sim \sum_{i,j} e^{-iq \cdot (R_i - R_j)} \exp \left[ -\frac{(\omega - \Omega_0)^2}{a^2(1 + \langle p_i p_j \rangle)} \right]. \quad (14)$$

Therefore, the width  $\Gamma_q$  of the peak around  $\omega = \Omega_0$  depends on the momentum  $q$  as  $\Gamma_q = \Gamma(q\xi_{CDT})$ , which increases about a factor of  $\sqrt{2}$  when  $q$  increases across  $q \sim \xi_{CDT}^{-1}$ . This  $q$  dependence of the Raman spectrum is expected to give the information on  $\xi_{CDT}$ , which should be different from  $\xi_{FT}$  when the system is near the gauge symmetric model, i.e., the limit of large degree of degeneracy.

In conclusion, the effect of the gauge field in the hydrogen-bonded ferroelectrics is very subtle. In the vicinity of the CDT, the gauge field suppresses the growth of the critical region by regulating the correlation length. Our theory provides a scheme to uncover the shadow of the gauge field as well as to realise the accompanying CDT by identifying the two

length scales  $\xi_{\text{FT}}$  and  $\xi_{\text{CDT}}$  near the ferroelectric phase transition. Finally, our theory may shed light on a possible gauge structure in the real ice, ice XI, the ferroelectric phase of ice. It is not only important in laboratories but also with astrophysical implications [14, 15]. A future research direction toward the understanding of the gauge structure in ice is needed to be explored.

The authors acknowledge the fruitful discussion with Y. Tokura. This work is supported by Grant-in-Aid for Scientific Research (Grants No. 24224009) from the Ministry of Education, Culture, Sports, Science and Technology of Japan, Strategic International Cooperative Program (Joint Research Type) from Japan Science and Technology Agency, and Funding Program for World-Leading Innovative RD on Science and Technology (FIRST Program) (NN). It is also supported by National Science Council of Taiwan under the grant: NSC 100-2112-M-002-015-MY3 (CHC). CHC is grateful for the travelling support from Center for Theoretical Sciences in National Taiwan University.

- 
- [1] J.C. Slater, J. Chem. Phys. **9**, 16 (1941).
  - [2] G. A. Samara, Ferroelectrics **71**, 161 (1987).
  - [3] G. A. Samara, Phys. Rev. Lett. **27**, 103 (1971).
  - [4] P. S. Peercy and G. A. Samara, Phys. Rev. B **8**, 2033 (1973).
  - [5] Y. Moritomo, et al., Phys. Rev. Lett. **67**, 2041 (1991).
  - [6] J. B. Kogut, Rev. Mod. Phys. **51**, 659 (1979).
  - [7] R. Savit, Rev. Mod. Phys. **52**, 453 (1980).
  - [8] L. Pauling, J. Am. Chem. Soc. **57**, 2680 (1935)
  - [9] C. Castelnovo, et al., Nature **451**, 42 (2007).
  - [10] K. A. Ross, et al., Phys. Rev. X **1**, 021002 (2011)
  - [11] N. Shannon, et al., Phys. Rev. Lett. **108**, 067204 (2012).
  - [12] Y. Okimoto, et al., J. Phys. Soc. Jpn. **74**, 2165 (2005).
  - [13] G. F. Reiter, et al., Phys. Rev. Lett. **89**, 135505 (2002)
  - [14] W. B. MaKinnon, et al., Bulletin of the American Astronomical Society **37**, 732 (2005)
  - [15] H. Fukazawa, et al., The Astrophysical Journal **652**, 57 (2006)